Characterization of Poly-Dispersed Paint Droplet Trajectories in Systems with an Electrostatic Rotary Bell Atomizer

S. Zhao[1], G. S. P. Castle[1], K. Adamiak[1], Hong-Hsiang (Harry) Kuo[2,*], Yar-Ming Wang[2] and Hua-Tzu (Charles) Fan[2]
[1]Dept. of Electrical and Computer Engineering, University of Western Ontario, London, Ontario, N6A 5B9, Canada,
[2] GM R&D Center, Warren, Michigan 48090, USA

Abstract

Charged poly-dispersed paint droplets can be produced by an electrostatic rotary bell atomizer. These droplets have different sizes and charge-to-mass ratios and thus experience mechanical and electrical forces that result in different trajectories. FLUENT software was used to determine the paint droplet trajectories and user-defined functions (UDF) were compiled to calculate the electrostatic field and the electrostatic forces acting on the charged droplets. Two methods of droplet size input were used, namely the multiple injection method and the Rosin-Rammler method, and droplet size distributions acquired from experiment were assumed. The droplet charge-to-mass ratios were considered to vary inversely with diameter. The paint droplet trajectories, the transfer efficiency and paint layer thickness distribution on a planar target surface were calculated. The results show that poly-dispersed charged sprays expand spatially which results in more uniform droplet deposition. The smaller droplets concentrate at the inner part of the spray due to shaping air entrainment, while larger ones are at the outer part due to their higher momentum. It was found that the droplet charging improves the transfer efficiency for all droplet size ranges because of the electrical attraction when the droplets approach the target. The paint thickness distribution patterns are displayed under charge and no charge conditions.

Introduction

Most atomizers used in industry produce a spectrum of droplet sizes ranging from a few to about 500 micrometers. For electrostatic atomizers, the droplets also have different charge-to-mass ratios for different droplet sizes which result in different trajectories due to mechanical and electrical forces. In automotive painting the paint droplet trajectories are directly related to surface uniformity and transfer efficiency, therefore, they need to be carefully controlled. For the electrostatic rotary bell (ESRB) atomizer, which is widely used in the automotive painting industry, it is important to optimize the droplet size distribution and charge in order to achieve higher mass transfer efficiency and better surface quality. Since there are many parameters affecting the painting process, such as the ESRB atomizer geometry, paint type and its physical properties, target geometry, atomizer-to-target distance, liquid paint flow rate, bell speed, shaping air flow rate and applied voltage, numerical modeling makes it possible to test the working conditions on the computer and experiments can then be used to verify the optimized result, so that time and money can be saved.

The physical processes in electrostatic painting using the ESRB atomizer include paint atomization and charging, droplet transport, deposition and adhesion. The models for these processes are still evolving. Elmoursi [1] first used a simple Laplace field model to study a bell type electrostatic painting system which showed the dependence of droplet trajectories on electrical parameters. Then the model was expanded to include the space charge of charged paint droplets [2]. The study showed that the space charge tends to enhance particle deposition and also causes the spray to expand. Ellwood and Braslaw [3] developed a finite-element model which included the continuous phase of the shaping air, discrete phase of the droplets and the electric field in which the droplet charge-to-mass was assumed to be constant. The results showed that the increase of electric field near the target enhances the paint deposition. Im [4] simulated the compressible turbulent flow of the shaping air and motion of the paint droplets. The electric field of the applied voltage was modeled and the resulting electrical forces on the droplets were calculated. However, the effect of the space charge formed by the charged droplets was not considered. Domnick and Ye [5] modeled a painting system with a high-speed rotary bell atomizer and a flat target. A poly-dispersed droplet size distribution was considered and the droplet charge-to-mass ratios were assumed to be 5% of the Rayleigh limit. Viti et. al. [6] modeled the painting process in an automotive painting booth with a single rotating cup atomizer. An average charge-to-mass ratio was assumed and the booth downdraft airflow was also included. The major challenge for the

modeling of the poly-dispersed droplets is to calculate the space charge density formed by the charged droplets which have different sizes and charge-to-mass ratios. Ye et. al. [7] calculated the space charge density for a poly-dispersed powder coating gun in which the average charge-to-mass ratio in each cell was calculated. The product of the average charge-to-mass ratio and the particle concentration yielded the space charge density. The same technique was used for liquid painting. However, the charge-to-mass ratio was assumed to be 5% of the Rayleigh limit for all size ranges due to the difficulty of measuring charge-to-mass ratios for each droplet size. Many of the past studies assumed that the charge-to-mass ratio is constant for all droplet sizes and this significantly affected the modeling results. Generally speaking, the smaller droplets tend to have a higher charge-to-mass ratio than the larger ones. This has a great effect on the trajectories of the droplets.

We have incorporated the Poisson equation into FLUENT [8] and used it to study the effects of operating parameters on the paint droplet trajectories [9] in which the droplet size distribution was assumed uniform. In the present study, the paint spray is considered poly-dispersed, i.e. the droplet size distribution is no longer uniform. The droplet charge-to-mass ratio is not constant, but inversely proportional to the droplet diameter. The space charge density is calculated as a sum of the charges of different sized droplets contained in a cell over its volume. This makes the modeling closer to the real process. Different techniques for the droplet injection and trajectory display will also be discussed.

Droplet Size and Charge-to-Mass Ratio

There are several ways to represent the drop size distributions: graphical diagrams, mathematical distribution functions and median diameters [10]. The graphical techniques include producing a histogram which shows the number of drops whose dimensions fall between certain size bands. Certain drop size distribution measurement devices, such as the Malvern Particle Sizer, provide weight percentage for each size band. These data can be directly entered into FLUENT software. Mathematical distribution functions can also be used to express the experimental results and provide a means of consolidating large amounts of data. These functions include normal, log-normal, Nukiyama-Tanasawa, Rosin-Rammler and upper-limit distributions. In FLUENT, Rosin-Rammler and log-Rosin-Rammler functions are used to characterize drop size distributions. In many engineering applications, it is convenient to use drop mean diameters which include surface mean diameter (SMD), volume mean diameter (VMD) and Sauter mean diameter (SaMD). However, no single parameter can completely define a drop size distribution. For electrostatic painting, where the droplet size plays an important role for the surface quality and transfer efficiency, it is necessary to have a detailed drop size distribution in order to study the trajectories of droplets with different sizes.

The droplet charge-to-mass ratios (q/m) are different for different size droplets. They are mainly decided by the atomizer type, charging method and applied voltage, bell rotating speed, liquid properties and flow rate. These data can only be acquired from experiment. For example, Bell and Hockberg [11] did a lot of experiments with a rotary bell atomizer and provided an empirical equation for the charge-to-mass ratio correlated to operation parameters such as the bell speed, the applied voltage and the paint resistivity. However, the charge-to-mass ratio calculated from this equation is an average value and does not include the droplet size distribution. Gemci [12] measured the q/m of individual droplets by using Phase Doppler Interferometery. The q/m is calculated based on the balance of electric force and air drag force for given individual droplet size and velocity as well as electric field intensity. The values of q/m are surprisingly high and need to be further verified. There is still a lot of work to be done to find the relationship between the droplet charge-to-mass ratio and atomizer operating parameters. In the present situation when experimental data are not available, it is reasonable to assume that the charge-to-mass ratios of the droplets are reciprocal to their diameters. When the q/m of a typical volume mean diameter (VMD) and the size distribution are known, the charge-to-mass ratio for each size range can be calculated.

Numerical Algorithm

The major issues with implementing the numerical algorithm for the modeling of the electrostatic paint process with poly-dispersed droplets are entering droplet size and charge-to-mass ratio distributions, and calculating the space charge density. The modeling of the shaping air flow, the droplet discrete phase and the electric field and coupling between them are the same as for mono-dispersed (uniform) droplets and this has been discussed in detail in [9].

(1) Input Droplet Size Distribution

The droplet size distribution is acquired from the experimental results. It can be entered into FLUENT in two different ways: (1) multiple injections with each having one droplet size and flow rate; (2) Rosin-Rammler distribution with parameters derived from the experimental data. In the first method, the experimental data of droplet size distribution can be directly entered and the modeling results of each size band can be independently displayed. In the second method, data input and user-defined functions (UDF) used to calculate the electric field and force are much

simpler, but the experimental data may not fit well with the Rosin-Rammler distribution. To demonstrate these two methods, an experimentally determined droplet size distribution is used as shown in Fig. 1. The corresponding number distribution is shown in Fig. 2. In the measured data, there are as many as 36 size bands; here only 15 size bands are used, as this is assumed to be sufficient for good accuracy of computer modeling.

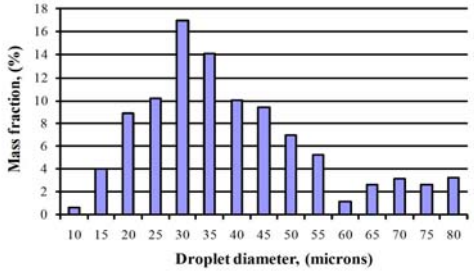

Fig. 1 Paint droplet size distribution with VMD of 35μm

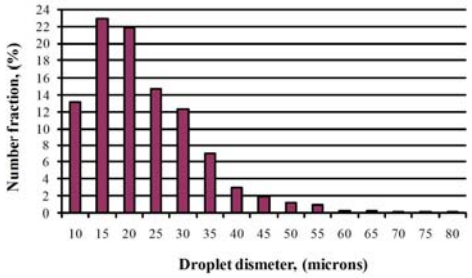

Fig. 2 Paint droplet number distribution with VMD of 35μm

A. Multiple injection method

This method uses one droplet size for each injection. The mass flow rate for each injection is derived from the mass fraction shown in Fig. 1. For a total number of 10,000 droplets in the model, the number for each size band is derived from Fig. 2.

B. Rosin-Rammler method

The Rosin-Rammler method assumes that the droplet size distribution obeys the following equation:

$$Y_d = e^{-(d/\bar{d})^n} \qquad (1)$$

where Y_d is the mass fraction of droplets with diameter greater than d, $\bar{d}$ is the mean diameter and n is the spread parameter. The method for calculating the mean diameter and the spread parameter is described in [13] and the calculated Y_d versus d is plotted in Fig. 3.

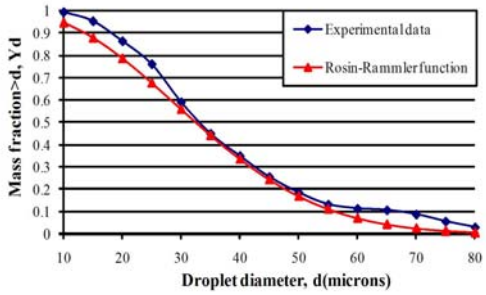

Fig. 3 Cumulative size distribution of the experimental data and the corresponding Rosin-Rammler function

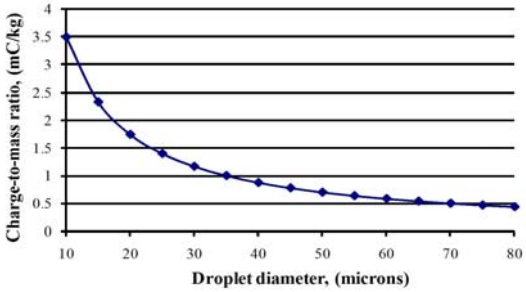

Fig. 4 Droplet charge-to-mass ratio distribution

The mean diameter $\bar{d}$ can be obtained from Fig. 3 assuming $Y_d = e^{-1}=0.368$ and this yields $\bar{d}$ =38.5μm. Then the spread parameter n is calculated which has an average value of n=2.2004. The obtained Rosin-Rammler distribution is compared with the experimental data in Fig. 3. Note that the mean diameter in Rosin-Rammler distribution is slightly different from the volume mean diameter (VMD) which is 38.5μm in this case. It can be seen from Fig. 3 that there are some differences between the experimental data and the Rosin-Rammler function.

(2)Input Droplet Charge-to-Mass Ratio Distribution

The droplet charge-to-mass ratio is a function of the drop size (diameter) and can be defined as discrete data or as a function of droplet size. The discrete data is used together with multiple injections of the droplet size distribution, while the function is used when droplet size distribution functions are used. When it is assumed that all the droplets have the same surface charge density, i.e. charge-to-mass ratio is reciprocal to their diameter, and that the 35μm droplet has a *q/m* of 1mC/kg, then the *q/m* of all other droplets can be calculated and the results are shown in Fig. 4.

(3)Calculation of Space Charge Density with Different Sizes and Charge-to-Mass Ratios

In FLUENT steady state model, the discrete phase should be considered as a stream of particles rather than large number of particles distributed throughout the domain. The space charge density in each cell can be directly calculated as:

$$\rho = \frac{1}{\delta V}\sum q_i = \frac{1}{\delta V}\sum (q/m)_i \bullet \dot{m}_i (t_{out} - t_{in}) \qquad (2)$$

where δV is the volume of a cell, $(q/m)_i$ is the charge-to-mass ratio of the particle with a specific size, t_{in} and t_{out} are the entrance and exit time of the particle stream for the cell, $\dot{m}_i$ is the flow rate of the particle stream.

Once the space charge density is calculated, the Poisson field and the electrostatic force on the charged droplets can be solved with the same technique as described in [8].

(4)Calculation of Transfer Efficiency and Spray Uniformity

The transfer efficiency (TE) is defined as the mass deposited on the target surface over the total mass delivered from the atomizer. For mono-dispersed droplets, TE can be calculated as the number of droplets deposited on the target over the total number of droplets ejected from the atomizer. However, for poly-dispersed droplets, different sized droplets have different mass, so TE is calculated as the sum of weighed mass transfer efficiencies for all droplets sizes, i.e.

$$TE = \sum TE_i \cdot m_{fi} \qquad (3)$$

where TE_i is the mass transfer efficiency of the *i-th* droplet and m_{fi} is the corresponding mass fraction. For the multiple injection method, TE of each droplet size can be calculated using the method for mono-dispersed droplets, while for the Rosin-Rammler method, TE cannot be directly calculated.

The paint build-up speed at the target surface can be directly acquired from FLUENT in terms of accretion rate, which is defined as [11]

$$R_{accretion} = \sum_{p=1}^{N_{particles}} \frac{\dot{m}_p}{A_{face}} \qquad (4)$$

where $\dot{m}_p$ is the particle stream mass flow rate and A_{face} is the surface area. Because of evaporation of water or organic solvent, the actual film thickness is not the same as the accretion rate but they are proportional. The spray uniformity on the target surface can be examined by displaying the calculated accretion rate.

Results and Discussion

The computational domain for the 2D axisymmetrical model of the investigated painting process is the same as in [9]. For the base case, the input parameters were: paint flow rate 360cc/min., bell speed 4,000rpm, applied voltage -80kV, shaping air volume flow rate 980 l/min. The paint droplet size and charge-to-mass ratio are shown above.

(1)Base Case with Multiple Injection Method

In the base case, the spray has a droplet size distribution as shown in Fig. 1 in which the volume mean diameter (VMD) is 35μm. The spray has a *q/m* distribution as shown in Fig. 4 in which for 35μm droplet the *q/m* is 1mC/kg. With the multiple injection method, the modeling results such as droplet spatial concentration, trajectories, transfer efficiency and surface uniformity are shown below. They are also compared with the results obtained for uncharged droplets.

A. Droplet spatial concentration

The droplet spatial concentrations under charge and no-charge conditions are shown in Figs. 5 and 6. In order to get a clearer view of the droplet spatial concentration, the maximum scale for the concentration is set at 0.5kg/m^3. The calculated maximum value is 2.736kg/m^3 and values greater than 0.5kg/m^3 can be seen near the center of the spray. It is shown that when the spray is charged, it expands radially due to electrostatic forces, which results in a more uniform distribution than with no charge. Also, more droplets are carried away by the air stream when droplets are not charged.

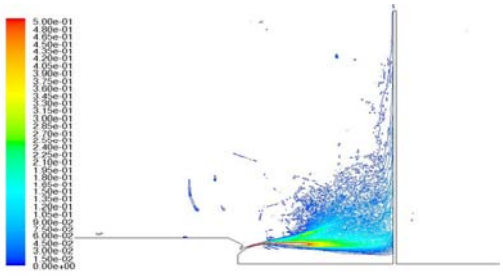

Fig. 5 Droplet concentration for charged spray (kg/m^3)

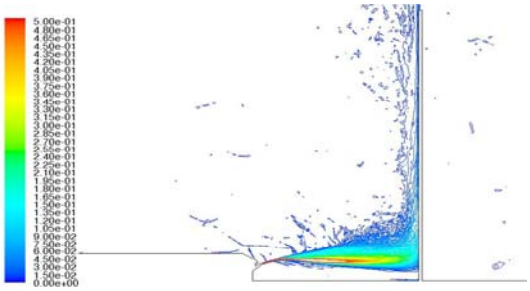

Fig. 6 Droplet concentration for uncharged spray (kg/m^3)

B. Droplet trajectories

The droplet trajectories under charge and no-charge conditions are shown in Figs. 7 and 8. In order to show clearly the droplet trajectories, only 100 droplets are displayed in the figures. It can be seen from the figures that the larger droplets are at the outer part of the spray due to their higher momentum, while the smaller ones are at the inner part of the spray due to the shaping air entrainment. That is one reason why the bell type atomizer has a higher mass transfer efficiency than other types of spray guns.

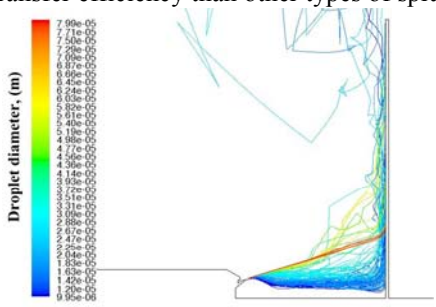

Fig. 7 Overall droplet trajectories (with charge)

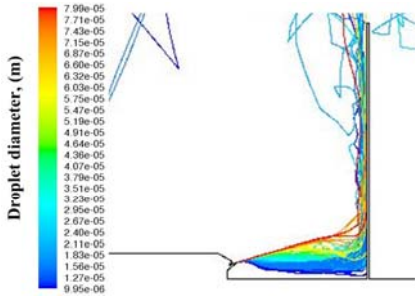

Fig. 8 Overall droplet trajectories (without charge)

C. Transfer efficiency

The transfer efficiency for the overall spray is 92% with charge and 84% without charge. For specific sizes the transfer efficiencies are illustrated in Fig. 9. The results show that for droplets of all size ranges the transfer efficiency improves when they are charged. For droplet diameters larger than 60μm, the results showed relative lower transfer efficiency with no charge and 100% transfer efficiency with charge. This is probably due to the fact that the mass and number fractions of these droplets are very small.

D. Coverage uniformity

The target surface coverage uniformity can be examined in terms the paint buildup speed (accretion rate) at the target surface. The paint accretion rates under charge and no-charge conditions are shown in Figs. 10 and 11. From the figures it can be seen that when droplets are charged, they tend to distribute more widely when approach to the target. Conversely, when the droplets are not charged, they distribute in a narrow area and the peak value is much higher than that with charge. The spray pattern can be adjusted by varying the bell rotating speed and shaping air flow rate as well as the applied voltage. The coverage uniformity is not only related to the spray pattern of a single stationary bell, but also is decided by the motion of the bell and multi-bell combinations. The spray pattern of the single bell provides the basis for further analysis.

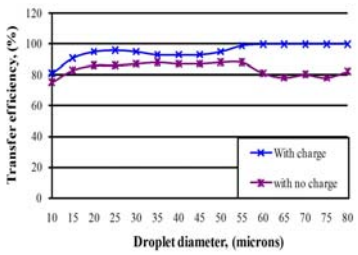

Fig. 9 Transfer efficiency under charge and no-charge conditions

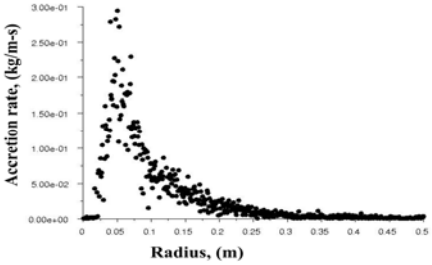

Fig. 10 Paint accretion rate for charged spray

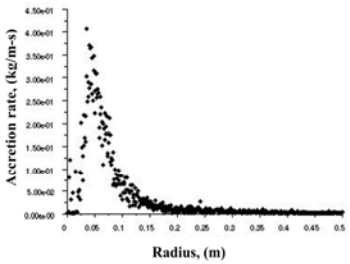

Fig. 11 Paint accretion rate for uncharged spray

E. Comparison with Rosin-Rammler Method

As an alternative method, the Rosin-Rammler distribution of droplet size was tested under the same operating conditions. Due to space considerations, only the droplet spatial concentration and trajectories are displayed in Figs. 12 and 13. Comparing with Fig. 5, the two methods showed basically the same trends. Since the Rosin-Rammler function does not exactly agree with the measured data, and the droplet size changes continuously, these two trajectory patterns are not exactly the same. Although the Rosin-Rammler method cannot display the trajectories of droplets with single sizes, it simplifies the entering of injection parameters and writing the UDFs, especially for 3D modeling.

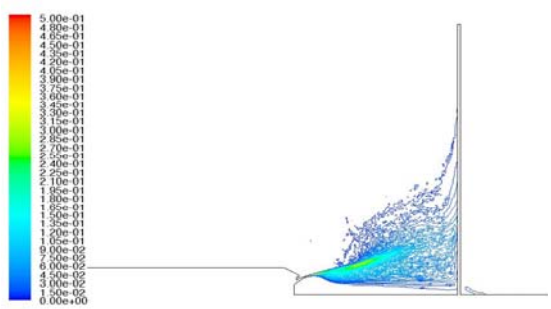

Fig. 12 Droplet concentration (kg/m^3) with charge using Rosin-Rammler distribution

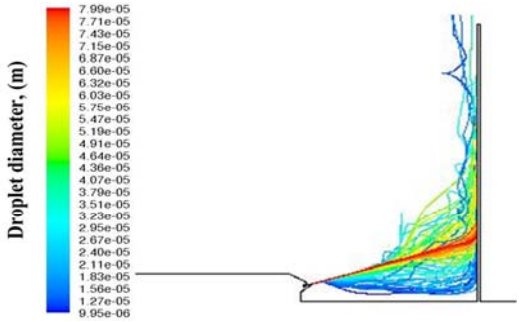

Fig. 13 Overall droplet trajectories using Rosin-Rammler method

Conclusion

The electrostatic painting process with the rotary bell atomizer has been modeled using FLUENT fluid dynamics software assuming poly-dispersed droplets. The droplet size distribution was adopted from the experimental data while the charge-to-mass distribution was assumed to be reciprocal to the droplet diameter. Two droplet injection methods, the multiple-injection and the Rosin-Rammler, were used and their differences were discussed. For each method, the user-defined functions (UDF) were compiled to calculate the electric field formed by the charged droplets and the electric force on the droplets. The paint droplet spatial concentration, trajectories, transfer efficiency and target surface coverage uniformity were studied with and without charge. The results showed that for poly-dispersed sprays, charged spray expands radially which results in more uniform droplet distribution; smaller droplets are at the inner part of the spray due to shaping air entrainment while larger ones are at the outer part due to their higher momentum; the transfer efficiency improves for all droplet size ranges because of the electrical attraction when they approach the target.

Acknowledgement

This project is partially supported by the Natural Sciences and Engineering Research Council of Canada (NSERC) and General Motors of Canada Limited.

References

1. Elmoursi, A.A., “Laplacian fields of bell-type electrostatic painting systems,” *IEEE Trans. Ind. Appl.*, vol. 25, pp. 234-240, 1989.
2. Elmoursi, A.A., “Laplacian fields of bell-type electrostatic painting systems,” *IEEE Trans. Ind. Appl.*, vol. 25, pp. 234-240, 1989.
3. Ellwood, K.R.J. and Braslaw, J., “A finite-element model for an electrostatic bell sprayer,” *J. Electrostatics*, vol. 45, pp.1-23, 1998.
4. Im, K.-S., Lai, M.-C, Yu, S.-T.J. and Matheson, R.R., “Simulation of spray transfer processes in electrostatic rotary bell sprayer,” *J. Fluids Eng.,* vol. 126, pp. 449-456, 2004.
5. Domnick, J., Scheibe, A. and Ye, Q., “The simulation of the electrostatic spraying painting process with high-speed rotary bell atomizers. Part I: direct charging,” *Part. Part. Syst. Charact.,* vol. 22, pp. 141-150, 2005.
6. Viti, V., Salazar, A. and Saito, K., “A numerical study of the coupling between the flow field and the electrostatic field inside an automotive spray paint booth,” *IASME Transactions*, vol. 2, pp.261-266, 2005.
7. Ye, Q., Steigleder, T., Scheibe, A. and Domnick, J., “Numerical simulation of the electrostatic powder coating process with a corona spray gun,” *J. Electrostatics*, vol. 54, pp.189-205, 2002.
8. Zhao, S., Adamiak, K. and Castle, G.S.P., “The implementation of Poisson field analysis within FLUENT to model electrostatic liquid spraying,” *2007 IEEE Canadian Conf. on Electrical and Computer Eng.*, Vancouver, British Columbia, Canada, paper W81-5, April 22-26, 2007.
9. Zhao, S., Adamiak, K., Castle, G.S.P., Kuo, H.-H. (Harry), Wang, Y.-M. and Fan, H.-T. (Charles), “Modeling the effects of operating parameters on the paint trajectories for an electrostatic rotary bell atomizer,” *6th Int. Conf. on Applied Electrostatics*, Shanghai, China, Nov. 3-7, 2008.
10. Lefebvre, A.H., *Atomization and Sprays*, New York: Hemisphere Publishing Co., 1989.
11. Ellwood, K. R. J. and Braslaw, J., "A finite-element model for an electrostatic bell sprayer," *J. Electrostatics*, vol. 45, 1998, pp.1-23.
12. Gemci, T., Hitron, R. and Chigier, N., “Measuring charge-to-mass ratio of individual droplets using phase Doppler interferometery,” *ILASS Americans*, *15th Annual Conf. on Liquid Atomization and Spray Systems*, Madison, WI, USA, May 2002, pp.241-245.
13. FLUENT 6.2 User’s Guide, Fluent Inc., 2005.